JTTEE5 20:195–204
DOI: 10.1007/s11666-010-9580-2
1059-9630/$19.00 © ASM International

Comparative Study of the Electrical Properties and Characteristics of Thermally Sprayed Alumina and Spinel Coatings

Filofteia-Laura Toma, Stefan Scheitz, Lutz-Michael Berger, Viktar Sauchuk, Mihails Kusnezoff, and Sven Thiele

(Submitted May 21, 2010; in revised form October 1, 2010)

In this study, APS and HVOF processes have been used to prepare alumina (Al_2O_3) and magnesium spinel ($MgAl_2O_4$) coatings designed for insulating applications. The electrical characteristics, i.e., dielectric strength and electrical resistance (electrical resistivity) were investigated using different methods: dielectric breakdown test, direct current (DC) measurements, and electrochemical impedance spectroscopy (EIS). The electrical resistance was measured at room temperature at different relative humidity (RH) levels (from 6% RH to 95% RH) as well as at 200 °C. The coating microstructure, phase composition, and water vapor sorption were studied. Differences in the electrical insulating properties due to the different coating system characteristics are discussed. Of the coatings and conditions investigated in this study, the HVOF spinel coatings showed superior dielectric breakdown strength and electrical resistance stability at high humidity levels.

Keywords Al_2O_3, dielectric strength, electrical resistivity, insulating properties, microstructure, phase composition, spinel ($MgAl_2O_4$), water vapor sorption

1. Introduction

Owing to its remarkable insulating properties, aluminium oxide (Al_2O_3) is widely used in industrial applications in the fields of high-voltage electrical devices and integrated electronic systems. Thermally sprayed alumina coatings with suitable dielectric properties have been prepared and tested for manufacturing of electrostatic chucks, discharge devices, ozonizer tubes, and insulating coatings for reliable high-temperature heater systems (Ref 1-6). The electrical resistivity of sintered alumina (α-Al_2O_3, corundum) at 20 °C is stated to be on the order of magnitude of 10^{12}-10^{13} Ω m (Ref 7, 8). At room temperature, different values for the volume resistivity of the plasma-sprayed Al_2O_3 coatings have been reported in the literature depending on the feedstock powder, the spray process, and the method used for the estimation of the resistivity: 10^{10}-10^{13} Ω m (Ref 2); 5×10^7-3×10^{10} Ω m (Ref 9); 4-13 $\times$ 10^{10} Ω m (Ref 6); and 10^{12} Ω m (Ref 10). A major difference between sintered alumina and thermally sprayed alumina coatings is that the latter are composed of different thermodynamically unstable forms of Al_2O_3 (e.g. γ- or δ-Al_2O_3) (Ref 11, 12), even though all commonly used feedstock powders consisted of α-Al_2O_3, the only stable modification of Al_2O_3. The properties of metastable Al_2O_3 phases differ significantly from those of corundum; i.e., γ-alumina has a higher hygroscopicity which is supposed to be deleterious to the dielectric properties of the material.

Sintered magnesium spinel ($MgAl_2O_4$) possesses good mechanical strength at room and high temperatures, high chemical inertness, good shock resistance, a low dielectric constant, and low electrical losses at microwave frequencies. It has a wide range of applications, for example, as a high-performance refractory material in furnace regenerators and radioactive waste confinements, a ceramic ultrafiltration membrane, an optical material, a catalyst, and a humidity sensor (see, e.g., Ref 13-16). The electrical resistance of spinel thin films decreases from 10^8-10^{11} to 10^6-10^9 Ω when the relative humidity increases from 2% to 98% (Ref 16). Relatively few studies have been published on the preparation of thermally sprayed spinel coatings (Ref 17-23). It has been shown that spinel is a stable compound during spraying and the coatings exhibit good mechanical properties. Electrical measurements have shown that they are good base dielectric materials at microwave frequencies (dielectric constant of ~6-8 in the

This article is an invited paper selected from presentations at the 2010 International Thermal Spray Conference and has been expanded from the original presentation. It is simultaneously published in *Thermal Spray: Global Solutions for Future Applications, Proceedings of the 2010 International Thermal Spray Conference*, Singapore, May 3-5, 2010, Basil R. Marple, Arvind Agarwal, Margaret M. Hyland, Yuk-Chiu Lau, Chang-Jiu Li, Rogerio S. Lima, and Ghislain Montavon, Ed., ASM International, Materials Park, OH, 2011.

Filofteia-Laura Toma, Stefan Scheitz, and **Lutz-Michael Berger**, Fraunhofer Institute for Material and Beam Technology (Fh-IWS), Winterbergstrasse 28, Dresden 01277, Germany; and **Viktar Sauchuk, Mihails Kusnezoff,** and **Sven Thiele**, Fraunhofer Institute for Ceramic Technologies and Systems (Fh-IKTS), Winterbergstrasse 28, Dresden 01277, Germany. Contact e-mail: filofteia-laura.toma@iws.fraunhofer.de.

as-sprayed state with loss tangent <0.005), electrical insulators in radiation environments and humidity sensors (Ref 20, 24). The electrical resistance of APS spinel coatings at very low humidity levels has been reported to be on the order of 10^9 Ω (Ref 24). Several authors (Ref 22, 23) proposed spinel coatings produced by vacuum plasma spraying as electrically insulating layers on metallic interconnectors in solid oxide fuel cells (SOFC). Nonetheless, thermally sprayed spinel coatings as insulating materials in electronic devices have been less extensively studied than alumina coatings.

This study is focused on the investigation of the electrical insulating properties of APS and HVOF thermally sprayed alumina and spinel coatings using different methods: dielectric breakdown test, direct current (DC) measurements, and electrochemical impedance spectroscopy (EIS). The effects of various factors, i.e., relative air humidity level, test temperature, microstructure, phase composition, and water adsorption, on the insulating properties of the coatings are presented and discussed.

2. Experimental Procedures

2.1 Materials and Coating Deposition

Commercial fused and crushed alumina (>99.7 wt.% purity) and magnesium spinel (Al_2O_3-28 wt.% MgO; >99.8 wt.% purity) powders (Ceram GmbH, Albbruck-Birndorf, Germany) with appropriate particle sizes for both APS (−40 + 10 μm) and HVOF (−25 + 5 μm) processes were used as the material feedstock for coating deposition. The chemical compositions of the feedstock powders are summarized in Table 1.

APS coatings were sprayed with an F6 Plasma Gun (6-mm nozzle, GTV mbH, Luckenbach, Germany) using an Ar/H_2 plasma gas mixture. HVOF coatings were sprayed with a Top Gun system (8-mm nozzle, GTV mbH) using ethylene as a fuel gas. The main spray parameters are summarized in Table 2. Coatings with average thicknesses of 100 and 200 μm were sprayed on grit-blasted mild steel (30 × 30 × 3 mm) and highly corrosion-resistant 1.4462 stainless steel plates (60 × 100 × 5.5 mm). The samples were then vacuum sealed in plastic films so that environmental contamination of the coatings during long-term storage could be minimized.

2.2 Coating Microstructures and Phase Compositions

The coating microstructures were examined by optical microscopy and scanning electron microscopy on metallographically polished cross sections. The phase compositions of powders and sprayed coatings were evaluated by x-ray diffraction using a D8 (Advance Bruker AXS) diffractometer. Measurements were carried out in the θ-2θ step scan mode using CuKα radiation and a step size of 0.05°. The phases were identified using the *Diffrac EVA software*. The volume content of the crystalline α-Al_2O_3 ($C_\alpha^{Al_2O_3}$) was determined using the following equation:

$$C_\alpha^{Al_2O_3}\ (\%) = \frac{A_\alpha(113)}{A_\alpha(113) + 0.89A_\gamma(400)} \times 100 \qquad \text{(Eq 1)}$$

where A is the integral area of the respective peak.

2.3 Investigation of Electrical Insulating Properties

Different methods were used to investigate the electrical insulating characteristics of the coatings: dielectric breakdown test, direct current (DC) measurements, and EIS.

The dielectric breakdown test allows for the determination of the dielectric breakdown voltage (DBV) and dielectric strength (E_d) of the coatings. The measurements were performed on as-sprayed coatings, without any surface finishing or sealing, at room temperature and room humidity through application of high DC voltages, using a PC6P testmeter (Sefelec GmbH, Ottersweier, Germany). The applied voltage was increased linearly at a rate of 100 V s^{-1} from zero to the occurrence of flashover. A silver paste was applied on the coating surface to provide a good electrical contact and to reduce the influence of the surface roughness. When the dielectric breakdown of the coating occurred, the dielectric breakdown voltage (DBV) was measured and the dielectric strength (E_d) was determined. For each sample (60 × 100 mm in size), measurements were made at nine points and the average value was calculated.

The electrical resistance/resistivity of the coatings was determined by direct current (DC) and alternating current

Table 2 Main spray parameters

APS	
Plasma gas mixtures Ar/H_2, slpm	35/13
Arc current, A	650
Plasma power, kW	59-60
Powder feed rate, g min^{-1}	26-30
Spray distance, mm	115
HVOF	
C_2H_4/O_2, slpm	90/270
Powder feed rate, g min^{-1}	27-30
Spray distance, mm	150

Table 1 Chemical compositions of feedstock spray powders (according to product certification data sheets)

Powder	Al_2O_3, wt.%	MgO, wt.%	TiO_2, wt.%	SiO_2, wt.%	Fe_2O_3, wt.%	CaO, wt.%	Na_2O, wt.%
Al_2O_3-APS	99.77	0.04	0.02	0.03	0.02	0.02	0.10
Al_2O_3-HVOF	99.74	0.04	0.02	0.03	0.03	0.01	0.13
Spinel-APS, Spinel-HVOF	71.61	28.22	0.02	0.04	0.02	0.09	…

(AC) methods at room temperature at different relative air humidity (RH) levels and at 200 °C (only for DC method). The DC electrical resistance of the as-sprayed samples was measured using an Advantest R8340 Ultra-high Resistance Meter (Advantest Corporation, Tokyo, Japan) through application of DC voltages of 50, 100, and 200 V. Silver paint was used as a contact material. EIS allows the electrical properties (impedance) to be determined as a function of frequency. The EIS measurements were performed with a Zahner IM6 Impedance Analyzer (Zahner-Elektrik GmbH & Co KG, Kronach, Germany) using a two-electrode cell. A stainless steel electrode with a diameter of 3.5 cm was used as the counter electrode, and the ground coating specimen as the working electrode. An alternating voltage with an amplitude of 5 mV at no DC bias in the frequency range from 100 kHz to 100 μHz was applied during the tests at room temperature. The contributions of the resistive and capacitive components of the overall total impedance can be estimated from these measurements. At high frequencies the capacitive character (dielectric properties) is predominant, whereas in the low-frequency domain the electrical resistance properties of the coatings are noticeable. The electrical resistance of the coatings could be determined through simple $R\|C$ equivalent circuit model fitting.

For investigation of the influence of the relative air humidity on the insulating properties, the samples were placed in a desiccator and conditioned for 48 h at different relative humidity levels ranging from 6% RH to 95-97% RH using saturated salt solutions. The electrical resistances were then determined by DC and EIS measurements using the same procedures as described above. The DC resistance of coatings at 200 °C was measured after pre-exposure of the samples for 2 h in the drying box maintained at the same temperature.

2.4 Dynamic Vapor Sorption (DVS) Measurements

Dynamic vapor sorption (DVS) allows for the determination of the mass changes during sorption/desorption cycles of water vapor on solid surfaces and investigation of different phenomena such as surface adsorption-desorption, bulk absorption, or hydration-dehydration. In surface adsorption, water interacts weakly with the surface by van der Waals forces (physisorption) or more strongly (chemisorption). Physisorption can be reversed through a decrease in humidity or an increase in temperature. Chemisorption is generally considered as irreversible. In bulk absorption, water is attracted deep into the internal structure of the material. Bulk absorption is reversible, but the kinetics in this case is slower than for surface adsorption. DVS measurements were performed using a DVS1 apparatus (Porotec GmbH, Hofheim, Germany) on spray powders and free-standing HVOF-sprayed coatings at 25 °C with humidity levels increasing from 0% RH to 95% RH. Before the tests were started, the samples (40-60 mg) were dried with gaseous N_2 (flow rate of 200 cm^3 min^{-1}) at 0% RH humidity until the mass was constant.

3. Results

3.1 Phase Compositions and Coating Microstructures

The alumina powders consisted mainly of the corundum phase, α-Al_2O_3 (JCPDS card No. 46-1212); traces of β-Al_2O_3 (JCPDS card No. 10-0414) could be detected. In the spinel powders, the cubic $MgAl_2O_4$ crystalline phase (JCPDS card No. 21-1152) and traces of MgO (JCPDS card No. 45-0946) were found in the HVOF powder.

Differences in the phase compositions of the alumina powders and coatings were found (Fig. 1a). The coatings contained the metastable phase γ-Al_2O_3 (JCPDS card No. 10-0425) as the main phase and α-Al_2O_3. The α-phase content was about 21 vol.% in the HVOF coating, but only 4 vol.% in the APS coatings. Spinel was found to be stable during spraying; the cubic $MgAl_2O_4$ structure found in the powders was the only phase identified in the coatings (Fig. 1b). This result was also confirmed by Mauer et al. (Ref 23) for spinel coatings produced by very low pressure vacuum plasma spraying (VLPPS).

The optical micrographs of the coatings are shown in Fig. 2. More dense microstructures appeared in the HVOF-sprayed coatings compared to those observed in the APS-sprayed coatings. In high-magnification SEM

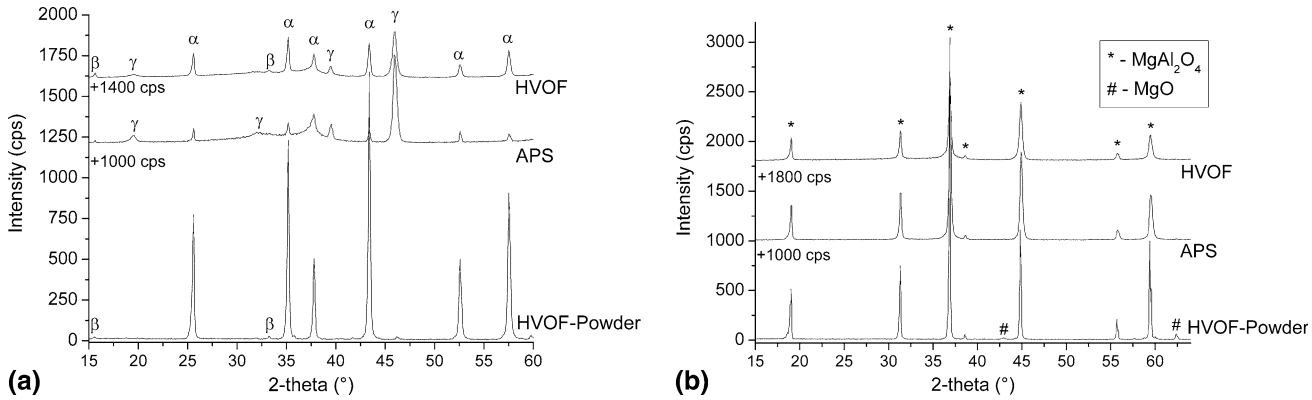

Fig. 1 XRD patterns of feedstock HVOF powders and thermally sprayed coatings: (a) Al_2O_3; and (b) spinel

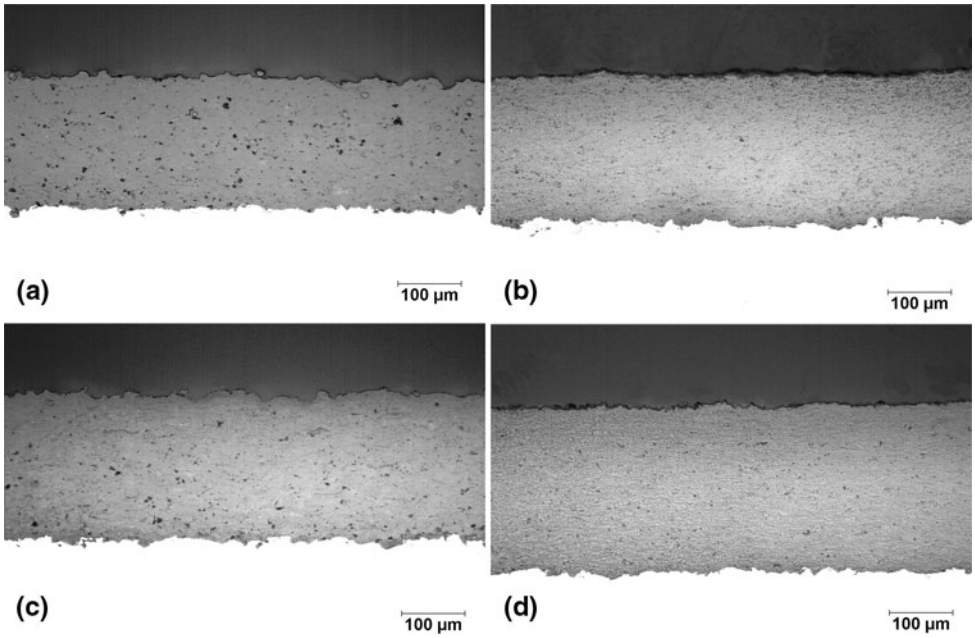

Fig. 2 Optical micrographs of thermally sprayed coatings: (a) Al_2O_3-APS; (b) Al_2O_3-HVOF; (c) Spinel-APS; and (d) Spinel-HVOF

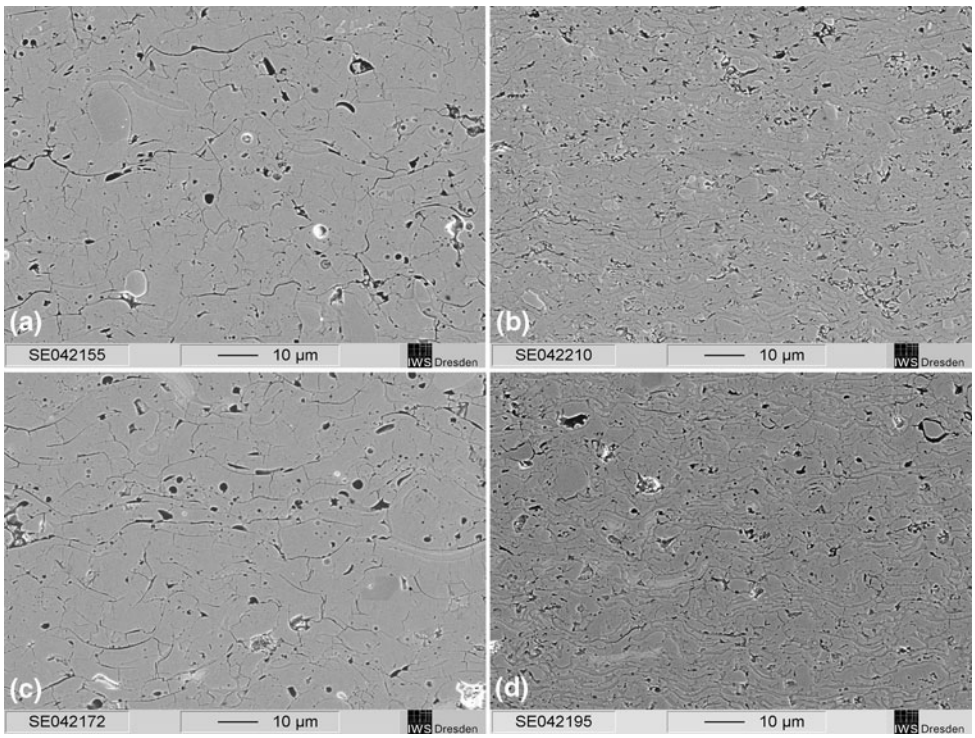

Fig. 3 Cross-sectional SEM micrographs of thermally sprayed coatings: (a) Al_2O_3-APS; (b) Al_2O_3-HVOF; (c) Spinel-APS; and (d) Spinel-HVOF

micrographs, the coatings showed the classical lamellar structure of thermally sprayed coatings, with the typical microstructural defects (porosity, cracks, unmelted particles, etc.) being observed (Fig. 3). The average porosity for both APS and HVOF coatings, estimated by image analysis on SEM micrographs at a magnification of 1000×, reached values between 4 and 9%. During the conditioning of the coatings sprayed on mild steel substrates at 95% RH the presence of brown spots on the coating surface, in particular for the APS coatings, indicated corrosion of the steel substrates, as can be seen in Fig. 4. It can be supposed that the APS coatings contained a higher content of

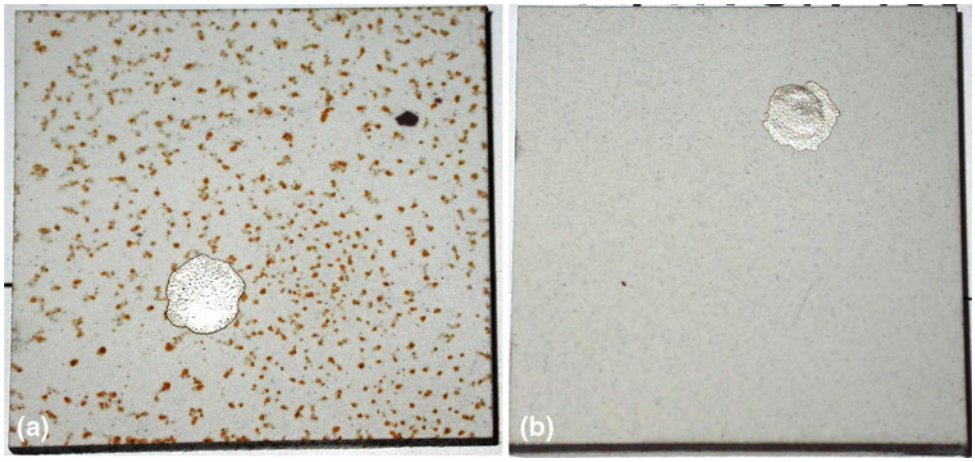

Fig. 4 State of the top-surfaces of spinel coatings sprayed on steel substrates after conditioning for 48 h at 95% RH: (a) an APS coating with 100-μm thickness; and (b) an HVOF coating with 100-μm thickness. The brown points on the coating surface indicate the substrate corrosion, while the wide spots represent the silver paste applied on the coating surface to provide a good electrical contact during the dielectric breakdown test. (Color figure online)

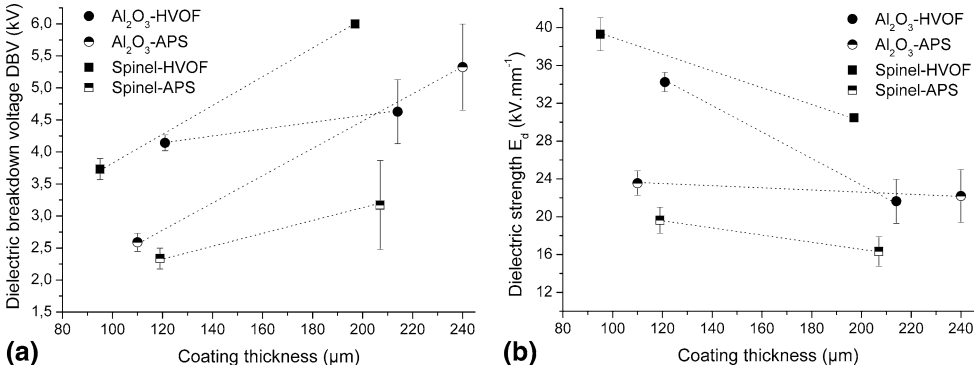

Fig. 5 Dielectric properties as a function of coating composition and coating thickness: (a) dielectric breakdown voltage; and (b) dielectric strength (dotted lines are for orientation purposes only)

Table 3 Average values of DC electrical resistance of sprayed coatings determined under different test conditions

Coating	Al_2O_3 (APS)		Al_2O_3 (HVOF)		Spinel (APS)	Spinel (HVOF)
Average thickness (μm)	100	200	100	200	100	200
R (Ω) at RT, ~30% RH	2.70×10^{11}	2.90×10^{11}	1.13×10^{11}	1.08×10^{11}	3.60×10^{11}	2.58×10^{11}
R (Ω) at RT, ~95% RH	4.44×10^{4}	2.24×10^{4}	3.76×10^{5}	3.16×10^{5}	3.18×10^{5}	5.55×10^{5}
R (Ω) at 200 °C	2.82×10^{10}	2.18×10^{10}	8.03×10^{10}	7.71×10^{10}	1.44×10^{10}	1.28×10^{11}

open porosity or interconnected porosity than the HVOF coatings.

3.2 Dielectric Breakdown Test

The average dielectric breakdown voltages (DBV) and dielectric strengths (E_d) of the sprayed coatings as a function of coating composition and coating thickness are shown in Fig. 5. The DBV increased, but the E_d decreased, with increasing coating thickness. The HVOF spraying method allows for the production of coatings with better dielectric properties than those prepared using the APS method. Moreover, for APS-sprayed spinel samples, the dielectric breakdown occurred at the lowest voltage values presenting a dielectric strength of below 20 kV mm^{-1}. The HVOF spinel coatings presented superior dielectric strengths to those of the HVOF alumina coatings: DBV $>$ 3.5 kV; E_d $>$ 30 kV mm^{-1}.

3.3 Electrical Resistance Measurements

DC electrical resistances of coatings with average thicknesses of 100 and 200 μm measured at room temperature in air at two different humidity levels (30% RH and 95% RH, respectively) and at 200 °C are shown in Table 3. The resistance values were found to depend on the measurement conditions, the spray method, and the coating material.

At the low air humidity level, the electrical resistances were on the order of 10^{11} Ω for both alumina and spinel coatings. Moreover the coating thickness was found to have almost no influence on the electrical resistance. At 95% RH, the electrical resistance decreased to values on the order of 10^4 Ω for plasma-sprayed Al_2O_3 coatings and 10^5 Ω for HVOF-sprayed Al_2O_3 and spinel coatings. HVOF-sprayed coatings were less sensitive to humidity than the APS coatings. At 200 °C, the electrical resistance was on the order of magnitude of 10^{10} Ω for alumina and APS spinel coatings, and on the order of magnitude of 10^{11} Ω for HVOF spinel coatings. In these tests, spinel coatings presented superior insulating properties to those of alumina coatings.

The EIS method was used to evaluate the electrical properties of coatings at room temperature as a function of humidity in a large frequency domain (Fig. 6). At low frequencies the impedance was relatively independent of frequency, showing purely resistive behavior. The coating resistance as a function of thickness can be more conveniently expressed as the electrical resistivity ρ which can be determined from the formula $\rho = (RS)/d$, where R is the resistance (impedance), S the exposed surface area, and d the coating thickness. The influence of relative humidities on coating impedance and electrical resistivity is shown in Fig. 7(a) and (b), respectively. For both materials and spray processes, the electrical resistance (resistivity) decreased almost linearly as the air humidity increased. HVOF-sprayed coatings exhibited slightly higher electrical properties as compared with the APS-sprayed counterparts. In the case of Al_2O_3 coatings, the values of the electrical resistances (resistivities) at 6% RH air humidity were about $4.33\text{-}6.83 \times 10^{10}$ Ω ($4.01\text{-}6.51 \times 10^{11}$ Ω m), and decreased to $4.0\text{-}9.50 \times 10^5$ Ω ($3.81\text{-}8.79 \times 10^6$ Ω m) at 97% RH air humidity. For spinel coatings, the electrical resistances (resistivities) decreased from $5.07\text{-}5.34 \times 10^{10}$ Ω ($1.78\text{-}3.19 \times 10^{11}$ Ω m) to 5.30×10^6 Ω ($1.86\text{-}3.17 \times 10^7$ Ω m) as the air humidity increased from 6% RH to 97% RH. At a high humidity, the spinel coatings still had a better insulation resistance than that of alumina coatings, which is in good agreement with the results previously obtained from DC measurements (see Table 3).

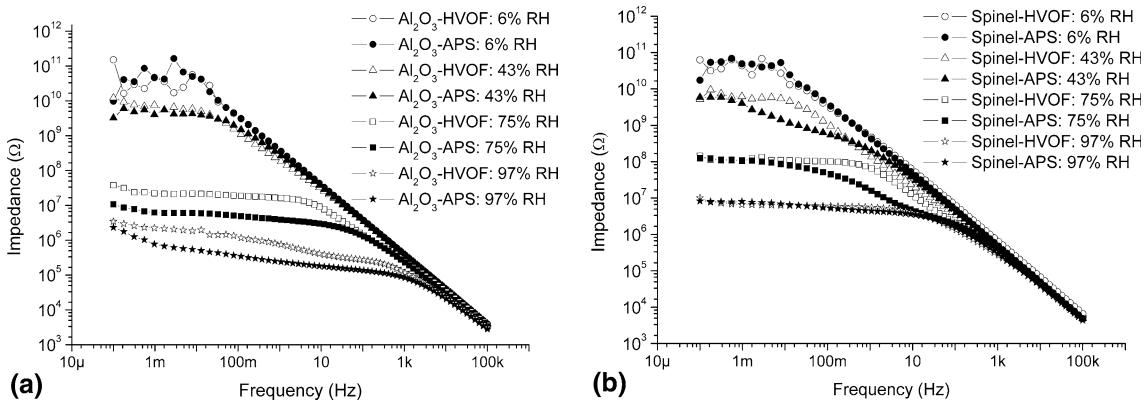

Fig. 6 Impedance as a function of frequency at different air humidity levels for (a) Al_2O_3; and (b) spinel coatings

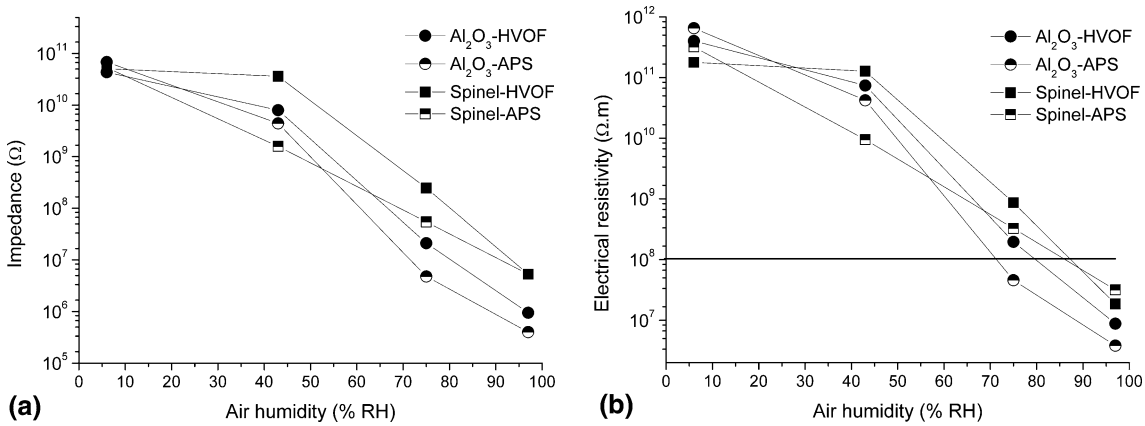

Fig. 7 Dependence of the impedance (a) and electrical resistivity; and (b) on relative air humidity level. For $\rho > 10^8$ Ω m, the materials are considered as insulators (Ref 25)

3.4 Dynamic Vapor Sorption (DVS) Measurements

DVS measurements were performed for determination and quantification of the interaction between the water vapor and the surface for oxide ceramics in the form of powders and coatings at room temperature, and humidity levels ranging from 0% RH to 95% RH. A rapid increase in water adsorption was recorded at 95% RH. In the case of the spray powders, the water vapor sorption at 95% RH was 0.08% for APS Al_2O_3 powder ($-40+10$ μm fraction), 0.17% for HVOF Al_2O_3 powder ($-25+5$ μm fraction), 0.76% for APS spinel powder ($-40+10$ μm fraction), and 1.78% for HVOF spinel powder ($-25+5$ μm fraction) (see Fig. 8). Mass changes were slightly higher for HVOF spray powders due to a higher contact surface area, and water sorption was more pronounced in the case of the spinel powders.

In the case of HVOF coatings, the water vapor sorption at 95% RH was 0.41% for Al_2O_3 and 0.30% for spinel (Fig. 9). The water sorption was higher on the Al_2O_3 coating than on the powders. Meanwhile, contrary to our expectations, a lower water sorption was recorded on the spinel coating than on the powder.

4. Discussion

4.1 Electrical Insulating Properties of the Spray Coatings

The dielectric strengths/dielectric breakdown voltages of the plasma-sprayed Al_2O_3 coatings obtained in this study were comparable with those reported in literature (see, for example, Friedrich et al. (Ref 4), Pawlowski (Ref 9) and Yamasaki and Takeuchi (Ref 10)). APS spinel coatings presented the lowest dielectric strength value; this result was also confirmed by Pawlowski (Ref 9). To the authors' knowledge, no information could be found in the literature on the dielectric strength values of the HVOF spinel coatings. The results of the dielectric breakdown tests showed better dielectric properties for the HVOF coatings than for the APS coatings which could be due to a lower open porosity (see Fig. 4). The presence of defects (porosity, cracks, etc.) should facilitate dielectric breakdown and coating failure.

It was observed that with increasing coating thickness, the DBVs increased, whereas the dielectric strength values decreased. This decrease in dielectric strength could

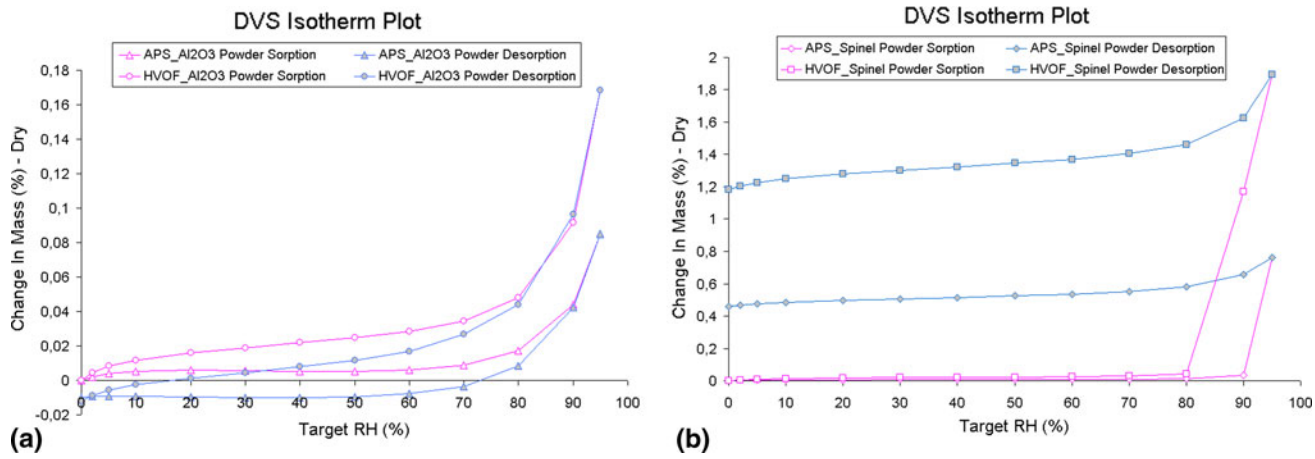

Fig. 8 Sorption/desorption cycles of water vapor on feedstock spray powders: (a) Al_2O_3; and (b) spinel

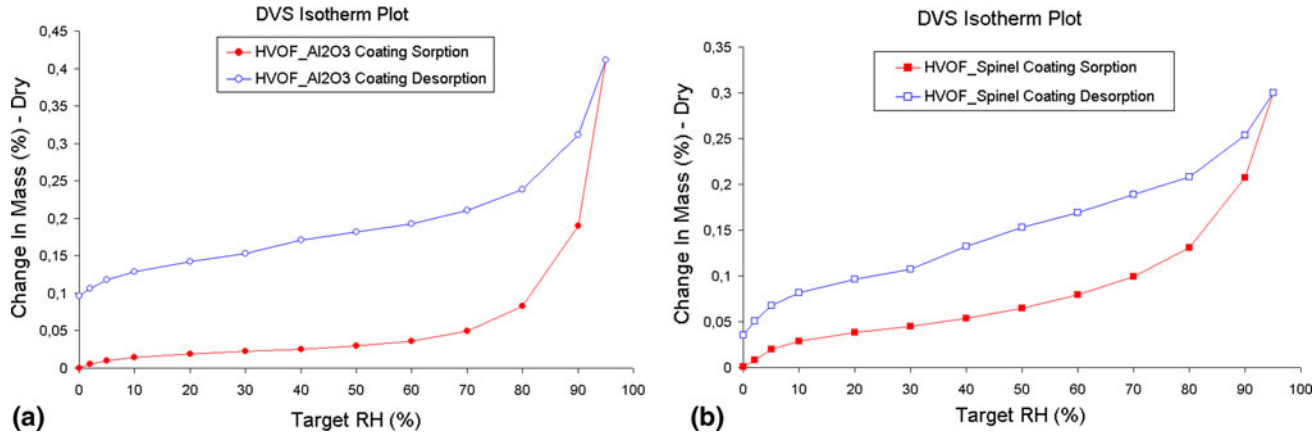

Fig. 9 Sorption/desorption cycles of water vapor on HVOF-sprayed coatings: (a) Al_2O_3; and (b) spinel

be explained by the heat/thermal mechanism (Ref 26). With increasing thickness, the puncture (the breakdown) will occur at a higher voltage (breakdown voltage). However, the electrical resistance increases more slowly than the thermal resistance of the sprayed coating. Thus, at high electric field densities, heat is generated at a rate faster through ionic conduction than that at which it can be dissipated in the coating volume. Breakdown may then occur because of local thermal instability in the material. Any internal coating defects (especially cracks and impurities) reduce the breakdown stability. Several authors (Ref 27, 28) have also confirmed that the dielectric breakdown is mainly based on the electrical discharges (corona) producing high local fields which typically include the surrounding medium.

From the DC electrical resistance and EIS measurements, the following conclusions were drawn:

- At low RH levels, the values of electrical resistivity were comparable for alumina and spinel coating materials (order of magnitude of 10^{11} Ω m).
- The electrical resistivity dramatically decreased in a highly humid (95% RH) environment: by about five orders of magnitude for alumina coatings and about four orders of magnitude for spinel coatings.
- HVOF coatings presented slightly better insulating properties than those of APS coatings, and HVOF spinel coatings showed the best results.

The electrical resistivities of APS alumina coatings (determined at low RH levels) were comparable with or even slightly higher than those reported by Pawlowski (Ref 9) and Prudenziati (Ref 6), but lower than those published by Swindeman et al. (Ref 2) and Yamasaki and Takeuchi (Ref 10). In this study, it was found that the electrical resistivity values of the APS spinel coatings were higher by an order of magnitude than those reported by Ahn et al. (Ref 24).

4.2 Dynamic Vapor Sorption (DVS) of Feedstock Powders and Sprayed Coatings

Dynamic vapor sorption (DVS) measurements performed on HVOF feedstock powders showed a rapid increase in the water adsorption at 95% RH. The water adsorption on the surface of oxide powders depends on the material, the particle sizes, and the presence of impurities resulting from the process of powder manufacturing. Compared with alumina powder, spinel feedstock powders (especially HVOF spinel feedstock powder) exhibited more pronounced water adsorption at high RH levels (see Fig. 8). An explanation for this could be that the HVOF spinel powder contained traces of free MgO (as identified by XRD analysis, as shown in Fig. 1b) which, due to the increase of the humidity, hydrolyzed to the very stable $Mg(OH)_2$ compound; consequently, a certain amount of water could be irreversibly retained during the DVS measurements, even at very low RH levels.

The DVS analysis performed on free-standing HVOF Al_2O_3 coatings showed a higher amount of water adsorbed in comparison with that of the feedstock powder. This can be explained by the presence of coating microstructural defects (cracks, porosity) and the metastable γ-phase which is more hygroscopic than the α-phase. The amount of water adsorbed on the spinel coating was less than that adsorbed on the alumina coating because of the very high stability of the spinel structure during spraying (same main phase as in spray powder). Contrary to the authors' expectations, a lower water sorption was recorded on the spinel coating than on the powder. A possible explanation for this could be the elimination of some impurities (including MgO which could not be found in the XRD pattern of the coating) during spraying. Nonetheless, more investigations must be carried out to gain a better understanding of this result.

4.3 Influence of Humidity and Coating Characteristics on Electrical Properties of Thermally Sprayed Coatings

The electrical (insulating) properties of the thermally sprayed alumina coatings are inferior compared with those published for sintered (bulk) alumina (Ref 7, 8). In the literature, this behavior is mainly explained by the presence of the metastable γ-phase, exhibiting a higher hygroscopicity than the stable α-phase, in the sprayed coatings. Moreover, a higher content of γ-Al_2O_3 and a porous microstructure are associated with pronounced degradation of the insulation behavior of thermally sprayed coatings (Ref 9).

In this study, the HVOF alumina coating had a higher α-phase content than the one produced by APS ($\alpha\text{-}Al_2O_{3(HVOF)}:\alpha\text{-}Al_2O_{3(APS)} = 5$) and, consequently, was expected to possess better insulating properties. The electrical measurements showed that at low humidity levels (<45% RH), the resistivities of the HVOF and APS alumina coatings were comparable. Only at higher humidity levels (>75% RH) were the differences between HVOF and APS coatings evident ($\rho_{HVOF}:\rho_{APS} = 2\text{-}4$). Nevertheless, for both coating types, the electrical resistivity decreased by about five orders of magnitude (Fig. 7) when the air humidity increased from 6% RH to 97% RH. In their study, Favre et al. (Ref 29) investigated the electrical properties of various α-Al_2O_3 powders as a function of relative humidity. Those authors showed that the resistivity of α-Al_2O_3 decreased linearly by several orders (by almost six orders) of magnitude when the humidity increased from 20 to 80%.

For spinel coatings, similar tendencies were found: insulating properties worsened with increasing relative humidity, although the spinel coatings were found to be less sensitive to moisture than the alumina coatings were. The electrical resistivity of spinel was reduced by four orders of magnitude when the air humidity increased from 6% RH to 97% RH. Other authors (Ref 16, 24, 30) had observed the same trend (i.e., a linear decrease in electrical resistance with increasing humidity) while measuring the insulating properties of spinel in the form of powders

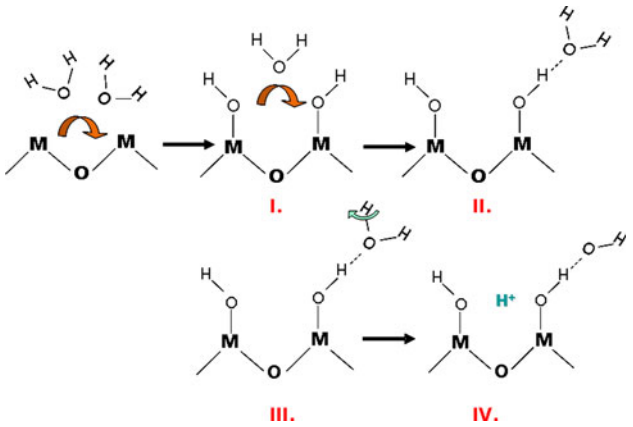

Fig. 10 Steps in the mechanism of water adsorption on the surface of a ceramic oxide: (I) Water chemisorption and formation of hydroxylated oxide surface; (II) Water physisorption; (III) Dissociation of physisorbed water; and (IV) Generation of protons (H^+) responsible for the ionic conduction

or plasma-sprayed coatings. Consequently, those authors proposed the use of spinel materials in the development of ceramic humidity sensors.

The deterioration of the electrical resistance with increasing humidity can be explained by the increase in surface electrical conductivity resulting from adsorption and accumulation of water monolayers on the surface of the oxide (Ref 31) and capillary condensation of the water in voids (pores, cracks). Capillary condensation depends both on the properties of the solid and the vapor; however, it is associated to mesopores which have an approximate size range from of 2-50 nm (Ref 32). Water adsorption is a natural physical phenomenon observed on every solid surface (Ref 33, 34). When a dry ceramic oxide is exposed to air humidity, a layer of water vapor molecules is first chemisorbed on the surface, resulting in the formation of a hydroxylated surface (Fig. 10). Subsequent layers of water molecules are physically adsorbed on hydroxyl layers. The easy dissociation of the physisorbed water, because of the high electrostatic field in the chemisorbed layer, produces protons which are responsible for the ionic electrical conduction (Ref 30). Moreover, the presence of coating imperfections such as cracks and porosity (especially of open porosity which is higher in the case of plasma-sprayed coatings) should have a detrimental effect on the electrical insulating properties. These coating imperfections generate the transverse channels for charge transfer, reducing the resistance of the coating. In this way, the electrical conductivity increases, and hence the insulating properties of the coating worsen. The sensitivity of the ceramic coatings to humidity is related to the nature of the material, the microstructure, and the phase composition.

5. Conclusions

A comparative study of the characteristics (microstructure, phase compositions, etc.) and the electrical insulating properties (dielectric strength and electrical resistance/resistivity) of APS and HVOF thermally sprayed alumina and magnesium spinel coatings was performed. Compared with Al_2O_3, spinel is a stable phase in the spray process. The effects of various factors, i.e., relative air humidity level and water vapor sorption, on the electrical properties of the coatings were investigated. At low humidity levels, the electrical resistivities of alumina and spinel coatings were comparable (on order of magnitude of 10^{11} Ω m). A dramatic decrease in resistivity of about five orders of magnitude for alumina coatings, and about four orders of magnitude for spinel coatings at a very high humidity (95% RH) was observed. This decrease was mainly due to the increase in water adsorption on the coatings, generating ionic conductivity. Of all the coatings investigated in this study, HVOF spinel coatings showed the best dielectric strength values ($E_d > 30$ kV mm^{-1}) and the lowest sensitivity to moisture. Thus, these coatings can be considered as potential candidates for use in insulating applications.

Acknowledgments

This study was part of the DKG (German Ceramic Society)/AiF research project ''Maßgeschneiderte keramische Schichtheizelemente, hergestellt durch thermisches Spritzen'' (Tailor-made ceramic coating heating elements obtained by thermal spraying), AiF No. 15.695BR, funded via AiF (Arbeitsgemeinschaft industrieller Forschungsvereiningungen) by the Federal Ministry of Economics and Technology. The authors gratefully acknowledge this funding. Thanks are also due to our colleagues Ms. B. Wolf for metallographic sample preparation, Ms. S. Raschke for SEM micrographs, and Ms. S. Saaro for XRD analysis.

References

1. R.T. Smyth and J.C. Anderson, Electronic Circuit Production by Arc Plasma Spraying, *Proc. 8th Int. Conf. Thermal Spraying*, Sept 27-Oct 1, 1976 (Miami Beach, FL), American Welding Society, 1976, p 456-463
2. C.J. Swindeman, R.D. Seals, W.P. Murray, M.H. Cooper, and R.L. White, An Investigation of the Electrical Behavior of Thermally Sprayed Aluminum Oxide, *Thermal Spray: Practical Solutions for Engineering Problems*, C.C. Berndt, Ed., ASM International, Cincinnati, OH, 1996, p 793-797
3. J. Takeuchi, R. Yamasaki, and Y. Harada, Development of a Low-Pressure Plasma Sprayed Ceramic Coating on Electrostatic Chucks for Semiconductor Manufacturing Equipment, *Proc. Int. Thermal Spray Conf.*, E. Lugscheider and C.C. Berndt, Ed., March 4-6, 2002 (Essen, Germany), DVS Verlag, 2002, p 960-964
4. C. Friedrich, R. Gadow, and A. Killinger, Thermally Sprayed Multilayer Coatings as Electrodes and Dielectrics in High Efficiency Ozoner Tubes, *Proc. United Thermal Spray Conf.*, E. Lugscheider and R. A. Kammer, Ed., March 17-19, 1999 (Düsseldorf, Germany), DVS Verlag, 1999, p 676-682
5. R. Gadow, A. Killinger, and C. Li, Plasma Sprayed Ceramic Coatings for Electrical Insulation on Glass Ceramic Components, *Proc. Int. Thermal Spray Conf.*, E. Lugscheider and C.C. Berndt, Ed., March 4-6, 2002 (Essen, Germany), DVS Verlag, 2002, p 213-219
6. M. Prudenziati, Development and the Implementation of High-Temperature Reliable Heaters in Plasma Spray Technology, *J. Therm. Spray Technol.*, 2008, **17**(2), p 235-243

7. W. Kollenberg, *Technische Keramik—Grundlagen, Werkstoffe, Verfahrenstechnik* (Engineering Ceramics—Fundamentals, Materials, Process Engineering), W. Kollenberg, Ed., Vulkan-Verlag, Essen, 2004, p 210 (in German)
8. M. Miyayama, K. Kuomoto, and H. Yanagida, Engineering Properties of Single Oxides, *ASM Engineered Materials Handbook*, Vol 4, ASM International, Materials Park, OH, 1991, p 748-757
9. L. Pawlowski, The Relationship between Structure and Dielectric Properties in Plasma-Sprayed Alumina Coatings, *Surf. Coat. Technol.*, 1988, **35**(3-4), p 285-298
10. R. Yamasaki and J. Takeuchi, Physical Characteristics of Alumina Coating Using Atmospheric Plasma Spraying (APS) and Low Pressure Plasma Spraying (VPS), *Thermal Spray Solutions: Advances in Technology and Applications*, on CD-ROM, May 10-12, 2004 (Osaka, Japan), DVS Verlag, 2004
11. R. McPherson, Formation of Metastable Phases in Flame- and Plasma-Prepared Alumina Coatings, *J. Mater. Sci.*, 1973, **8**(6), p 851-858
12. C.C. Stahr, S. Saaro, L.-M. Berger, J. Dubsky, K. Neufuss, and M. Herrmann, Dependence of the Stabilization of α-Alumina on the Spray Process, *J. Therm. Spray Technol.*, 2007, **16**(5-6), p 822-830
13. A. Ghosh, R. Sarkar, B. Mukherjee, and S.K. Das, Effect of Spinel Content on the Properties of Magnesia-Spinel Composite Refractory, *J. Eur. Ceram. Soc.*, 2004, **24**(7), p 2079-2085
14. L. Thomé, A. Gentilsa, J. Jagielskic, F. Garridoa, and T. Thomé, Radiation Stability of Ceramics: Test Cases of Zirconia and Spinel, *Vacuum*, 2007, **81**(10), p 1264-1270
15. N.M. Khalil, M.B. Hassan, E.M.M. Ewais, and F.A. Saleh, Sintering, Mechanical and Refractory Properties of MA Spinel Prepared via Co-Precipitation and Sol-Gel Techniques, *J. Alloys Compd.*, 2010, **496**(1-2), p 600-607
16. G. Gusmano, G. Montesperelli, E. Traversa, A. Bearzotti, G. Petrocco, A. D'amico, and C. Di Natale, Magnesium Aluminium Spinel Thin Film as a Humidity Sensor, *Sens. Actuators B Chem.*, 1992, **7**(1-3), p 460-463
17. C. Petot, M. Ducos, and G. Petot-Ervas, Thermal Spray Spinel Coatings on Steel Substrates: Influence of the Substrate Composition and Temperature, *J. Eur. Ceram. Soc.*, 1995, **15**(7), p 637-642
18. G. Lallemand, S. Fayeulle, D. Treheux, and C. Esnouf, Microstructure Study of Spinel Plasma Coatings, *Thermal Spray: Meeting the Challenge of the 21st Century*, C. Coddet, Ed., ASM International, Nice, France, 1998, p 599-604
19. G. Bertrand, C. Meunier, P. Bertrand, and C. Coddet, Dried Particle Plasma Spray In-Flight Synthesis of Spinel Coatings, *J. Eur. Ceram. Soc.*, 2002, **22**(6), p 891-902
20. S. Sampath, J. Longtin, R. Gambino, H. Herman, R. Greelaw, and E. Toremy, Direct-Write Thermal Spraying of Multilayer Electronics and Sensor Structures, *Direct-Write Technologies for Rapid Prototyping Applications*, A. Pique and D. Chrisey, Ed., Academic Press, New York, 2002, p 261-302
21. H. Samadi and T.W. Coyle, Mapping Deposition Parameters and Microstructures of Plasma Sprayed Spinel, *Thermal Spray 2006: Building on 100 Years of Success*, on CD-ROM, B.R. Marple, M.M. Hyland, Y.-C. Lau, R.S. Lima, and J. Voyer, Ed., May 15-18, 2006 (Seattle, WA), ASM International, 2006
22. J. Arnold, S.A. Ansar, U. Maier, and R. Henne, Insulating and Sealing of SOFC Devices by Plasma Sprayed Ceramic Layers, *Thermal Spray 2008: Thermal Spray Crossing Borders*, on CD-ROM, E. Lugscheider, Ed., June 02-04, 2008 (Maastricht, The Netherlands), DVS Verlag, 2008, p 95-99
23. G. Mauer, R. Vaßen, and D. Stöver, Thin and Dense Ceramic Coatings by Plasma Spraying at Very Low Pressure, *J. Therm. Spray Technol.*, 2010, **19**(1-2), p 495-501
24. K. Ahn, B.W. Wessels, and S. Sampath, Spinel Humidity Sensors Prepared by Thermal Spray Direct Writing, *Sens. Actuators B Chem.*, 2005, **107**(1), p 342-346
25. E. Ivers-Tiffée and W. von Münch, *Werkstoffe der Elektrotechnik* (Electrotechnical Materials), 10th ed., B.G. Teubner Verlag/GWV Fachverlage Wiesbaden, 2007, p 142 (in German)
26. H.-J. Kim, S. Odoul, C.-H. Lee, and Y.-G. Kweon, The Electrical Insulation Behaviour and Sealing Effects of Plasma Sprayed Alumina-Titania Coatings, *Surf. Coat. Technol.*, 2001, **140**(3), p 293-301
27. F. Hövelmann, *Hochspannungstechnik-Elektrische Festigkeit Teil 2: Durchschlag gasförmiger, flüssiger und fester Isolierstoffe* (Fernstudienbrückenkurse: Studiengang Elektrische Energietechnik), Vol 1, Technische Fachhochschule Berlin, 1993 (in German)
28. E. Rajamäki, T. Varis, A. Kulkarni, A.J. Gutleber, A. Vaidya, M. Karadge, S. Sampath, and H. Herman, Parameter Optimization of HVOF Sprayed Alumina and Effect of the Spray Parameters on the Electrical Properties of the Coatings, *Proc. Int. Thermal Spray Conf.*, E. Lugscheider and C.C. Berndt, Ed., March 4-6, 2002 (Essen, Germany), DVS Verlag, 2002, p 622-626
29. F. Favre, F. Villieras, Y. Duval, E. McRae, and C. Rapin, Influence of Relative Humidity on Electrical Properties of α-Al_2O_3 Powders: Resistivity and Electrochemical Impedance Spectroscopy, *J. Colloid Interface Sci.*, 2005, **286**(2), p 615-620
30. A. Laobuthee, S. Wongkasemjit, T. Traversa, and R.M. Laine, $MgAl_2O_4$ Spinel Powder from Oxide One Pot Synthesis (OOPS) Process for Ceramic Humidity Sensors, *J. Eur. Ceram. Soc.*, 2000, **20**(2), p 91-97
31. B.-D. Yan, S.L. Meilink, G.W. Warren, and P. Wynblatt, Water Adsorption and Surface Conductivity Measurements on α-Alumina Substrates, *IEEE Trans. Components Hybrids Manufact. Technol.*, 1987, **CHMT-10**(2), p 247-251
32. F. Rouquerol, J. Rouquerol, and K. Sing, *Adsorption by Powders and Porous Solids. Principles, Methodology and Applications*, Academic Press, 1999, 467 p
33. V.E. Henrich and P.A. Cox, *The Surface Science of Metal Oxides*, Cambridge University Press, 1996, 464 p
34. M.A. Henderson, The Interaction of Water with Solid Surfaces: Fundamental Aspects Revisited, *Surf. Sci. Rep.*, 2002, **46**(1-8), p 5-308